nature neuroscience

Attentional modulation of human auditory cortex

Christopher I Petkov[1], Xiaojian Kang[2], Kimmo Alho[3], Olivier Bertrand[4], E William Yund[2] & David L Woods[1,2,5,6]

Attention powerfully influences auditory perception, but little is understood about the mechanisms whereby attention sharpens responses to unattended sounds. We used high-resolution surface mapping techniques (using functional magnetic resonance imaging, fMRI) to examine activity in human auditory cortex during an intermodal selective attention task. Stimulus-dependent activations (SDAs), evoked by unattended sounds during demanding visual tasks, were maximal over mesial auditory cortex. They were tuned to sound frequency and location, and showed rapid adaptation to repeated sounds. Attention-related modulations (ARMs) were isolated as response enhancements that occurred when subjects performed pitch-discrimination tasks. In contrast to SDAs, ARMs were localized to lateral auditory cortex, showed broad frequency and location tuning, and increased in amplitude with sound repetition. The results suggest a functional dichotomy of auditory cortical fields: stimulus-determined mesial fields that faithfully transmit acoustic information, and attentionally labile lateral fields that analyze acoustic features of behaviorally relevant sounds.

When subjects attend to sounds in a noisy environment, event-related brain potentials (ERPs)[1,2] and fMRI signals[3,4] show enhanced activity in auditory cortex. Auditory ERP studies have suggested that two processes contribute to these ARMs. First, attention amplifies SDAs produced by nonattended auditory signals. For example, attention enhances brief, phasic responses in auditory cortex[5], including those with tonotopically organized generators[6,7]. In addition, ERP studies suggest that attention activates regions of auditory cortex that respond weakly or not at all to unattended tones[8].

Previous brain imaging studies have observed attentional modulations in auditory cortex[9] but have not directly imaged ARMs or mapped their relationship to SDAs. Some fMRI studies have found larger responses to attended stimuli in both mesial and lateral auditory cortical fields (ACFs)[10], whereas others have reported enhanced responses primarily in lateral ACFs[11,12]. Part of the difficulty arises from the fact that different studies have not always controlled task difficulty and response density, so that differences in memory load, arousal or task complexity may contribute differentially to activations in 'attend' and 'ignore' conditions. In addition, different stimuli are sometimes presented in different attention conditions[11,12], leaving open the possibility that attention-related differences might include contributions from differential stimulus-feature tuning of different ACFs[13,14]. Finally, many previous studies compared primarily the extent of activations during attend-auditory and control conditions, an approach that is insensitive to attention-related enhancements in areas that are already excited by nonattended stimuli.

Ambiguities in the relationship between ARMs and SDAs leaves unresolved the question of whether ARMs primarily reflect an amplification of SDAs, thus sharing tuning properties with SDA generators (as would be predicted on the basis of visual attention studies[15]), or primarily reflect the addition of activity in ACFs not activated by nonattended sounds (as would be implied from previous ERP studies).

In the current experiment, we used an ERP-like experimental design that permitted the isolation of SDAs and ARMs in response to identical sounds, and used visual and auditory attention conditions that placed similar demands on memory, arousal and motor response. In addition, we used cortical surface mapping techniques[16–18] to visualize the distributions of ARMs and SDAs. We mapped ARM and SDA distributions as a function of sound frequency, sound location and sound repetition in order to elucidate the tuning properties of the neuronal populations giving rise to these responses. Our results suggest that attention differentially amplifies activations in lateral ACFs with tuning properties that emphasize different signal features than those reflected in SDAs.

RESULTS

Nine subjects performed auditory or visual discriminations in alternating 20-s blocks cued by a letter at fixation (**Fig. 1**). Two-thirds of the blocks contained both visual and auditory stimuli, and one-third contained unimodal stimuli (either visual or auditory). We isolated SDAs by subtracting auditory cortex activations during a difficult visual attention task without auditory signals from activations during the same task with added sounds. This procedure was designed to assure that SDAs reflected automatic sensory processing by minimizing covert auditory attention. ARMs were isolated by subtracting auditory cortex activations during bimodal attend-visual conditions from activations to the same bimodal sequences in attend-auditory conditions. SDA and ARM amplitudes and distributions were examined as a function of

[1]Center for Neuroscience, UC Davis, 1544 Newton Court, Davis, California 95616, USA. [2]Human Cognitive Neurophysiology Laboratory, UC Davis and VANCHCS, 150 Muir Road, Martinez, California 95553, USA. [3]Department of Psychology, University of Helsinki, Siltavuorenpenger 20 D, FIN-00014, Finland. [4]Mental Processes and Brain Activation Lab, INSERM U280, 151, cours Albert Thomas, 69424 Lyon, cedex 03, France. [5]UC Davis Department of Neurology, 4860 Y Street, Suite 3700, Sacramento, California 95817, USA. [6]UC Davis Center for Mind and Brain, 202 Cousteau Place, Suite 201, Davis, California 95616, USA. Correspondence should be addressed to D.L.W. (dlwoods@ucdavis.edu).

Published online 23 May 2004; doi:10.1038/nn1256

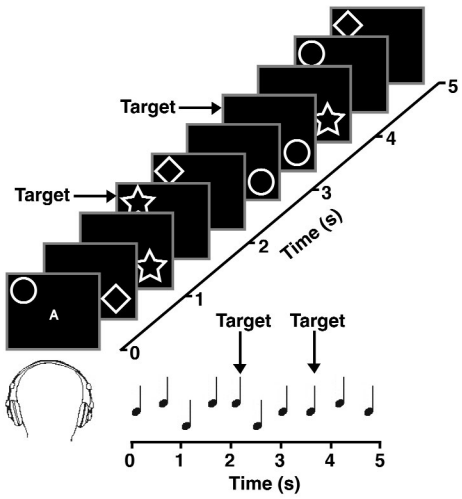

Figure 1 Behavioral task. Auditory and visual stimuli were presented at high rate while attention was cued to a modality in successive 20-s blocks by the letter "A" or "V": see text for further details.

sound frequency and location, and their adaptation was examined over 20-s stimulus blocks.

Auditory stimuli were either three different tones or three different narrow-band noise bursts (four semitones wide) presented at a location (left or right ear) and center frequency (350, 1,400 or 4,500 Hz) that remained constant throughout a block. The three sounds spanned an eight-semitone range (+4, 0 and –4 semitones) around the center frequency. Center frequency, sound type and sound location varied randomly across blocks. Sounds were presented randomly at a rapid rate (2/s), with the constraint that sound repetitions ('targets') occurred with an average probability of 13%. Visual stimuli were presented at the same rapid rate and with the same probability of repetition as auditory stimuli. Subjects responded with a button press to signal repetitions in the attended modality.

Functional activations were projected onto a high-resolution map of auditory cortex created by warping auditory cortical flat-patches from individual subjects using five local anatomical fiducial points (**Fig. 2a,b**). This technique produces a population map with preserved average auditory cortical gyral anatomy (**Fig. 2c**, also see **Supplementary Fig. 1** and **Supplementary Table 1** online) and reduced anatomical smearing in comparison with whole-brain normalization methods (Kang, X.J. *et al.*, Local functional mapping of human auditory cortex, *Proc. ISMRM*, May 18–24, 2002). fMRI images of blood oxygen level–dependent (BOLD) signals were obtained using conventional procedures and projected onto this map to show 'mean' functional activity.

The data were analyzed as mean percentage signal changes on a Heschl's/Planum (HP) grid that covered Heschl's gyrus and the planum temporale immediately posterior to it. The grid contained 3 × 3 mm grid elements and spanned approximately 30 × 42 mm (HP, dark blue dashed outline in **Fig. 2c**). Activations in this grid were statistically analyzed using 6-way repeated measures analysis of variance (ANOVA) with the following factors: sound frequency (low, medium, high), sound type (tone, noise), sound location (left, right ear), hemisphere (left, right) and mesiolateral (M-L) and anteroposterior (A-P) locations of the grid. Greenhouse-Geisser (ε) corrections were used when appropriate. To analyze the extent of significant activations, effects reaching statistical significance in the HP grid were further examined on six additional smaller grids (dimensions 15 × 21 mm) covering the superior and middle temporal lobe. In addition, activations were statistically analyzed in the four small grids that were included in the HP array (**Fig. 2c**).

Performance

The tasks were difficult (mean hit rate, 78%). Although auditory and visual conditions had been equated for difficulty in pilot studies, performance during the actual experiment was better for the auditory task (hit rate, 84% vs. 72%; $F_{1,8} = 8.39$, $P < 0.05$). Reaction times were also faster in auditory than in visual conditions (602 vs. 647 ms; $F_{1,8} = 6.98$, $P < 0.05$).

Sensory activations and attentional enhancements

Highly significant SDAs occurred within the HP grid (**Fig. 3a**, ANOVA; $F_{1,8} = 187.8$, $P < 0.001$) and over widespread regions of the superior and superior-lateral surface of the temporal lobe: significant SDAs were found in all but the two most posterior small grids (*i.e.*, grids I and J in **Fig. 3a**). Maximal SDAs occurred along the superior temporal gyrus (STG), slightly posterior to its intersection with Heschl's gyrus. Large activations were also evident in mesial Heschl's gyrus (grid E, $F_{1,8} = 57.9$, $P < 0.001$) in the vicinity of primary auditory cortex[19].

Significant ARMs were found in the HP grid ($F_{1,8} = 5.6$, $P < 0.05$) but were primarily restricted to lateral HP regions (**Fig. 3b**). In contrast to the widespread distribution of SDAs, significant ARMs were observed only in lateral grids (grids A, C, F and G, $P < 0.05$). In general, SDAs were more widespread than ARMs, and most regions

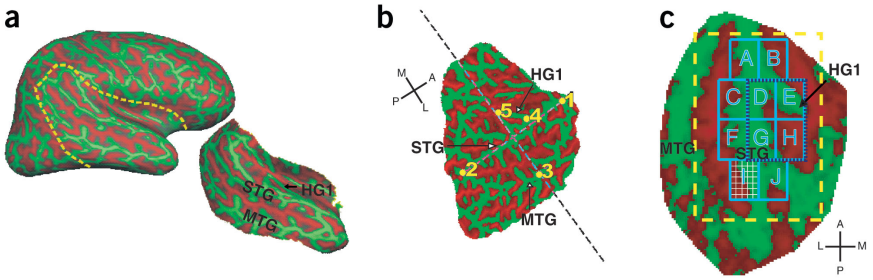

Figure 2 Imaging technique. (**a**) Each hemisphere was inflated and patches were cut that included the superior temporal and inferior parietal regions as shown on the right hemisphere of one subject. Surface curvature is color-coded (gyri = green, sulci = red). Abbreviations: HG1, Heschl's gyrus anterior (also see **Supplementary Fig. 1**); STG, superior temporal gyrus; MTG, middle temporal gyrus. (**b**) Auditory cortical patches were flattened and five local anatomical fiducial points (yellow circles) were selected for normalization: (1) anterior and (2) posterior junctions or extrapolated junctions of the STG and MTG; (3) Midpoint on the MTG; (4) The intersection of HG1 and the STG; (5) Mesial endpoint of HG1. These fiducial points were used to create an average map of auditory cortex with a common coordinate system by rotation and affine (linear) warping. M = mesial, L = lateral, A = anterior, P = posterior. (**c**) fMRI-BOLD signals were projected onto the normalized anatomical map (shown with group-averaged surface curvature measurements) and quantified on a grid with 3 × 3 mm elements (white boxes in grid I). Data from the Heschl's gyrus/planum temporale array (HP grid, dashed dark blue line) were analyzed using analysis of variance (ANOVA) for repeated measures. Ten smaller grids on the surface of the superior temporal lobe (A–J) were also analyzed. The dashed yellow line shows the area displayed in subsequent figures.

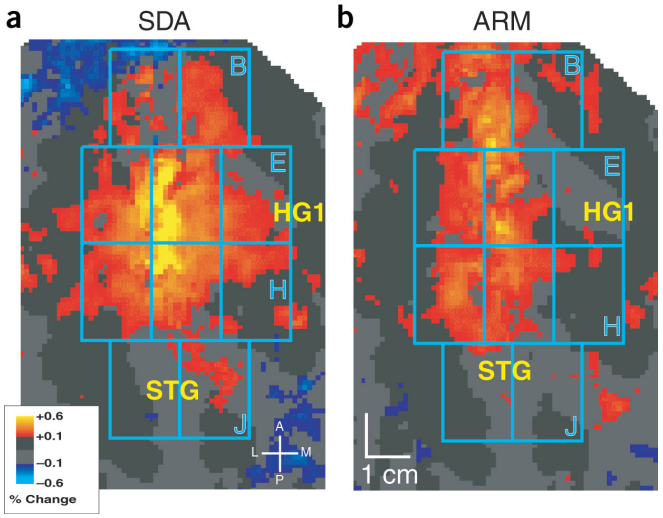

Figure 3 Stimulation-dependent activations and attention-related modulations (SDAs and ARMs). (**a**) SDAs reflecting the difference between visual attention conditions with and without auditory signals, co-registered onto normalized maps of auditory cortex (gyri = light gray, sulci = dark gray). Red/yellow colors indicate activation magnitudes. Shown are the outlines of the ten analysis grids (A–J; only grids B, E, H and J are labeled). Significant SDAs were obtained in all but the two most posterior grids. See **Figure 2c** for further details. (**b**) Attention-related modulations (ARMs): the difference between activations in auditory and visual attention conditions with identical bimodal stimulation. Significant ARMs were not observed in any of the mesial grids (B, E, H).

showing significant ARMs also had significant SDAs. However, in a few lateral regions (*e.g.*, grid A) ARMs appeared more prominent than SDAs. In contrast to SDAs, there was no evidence of ARMs in mesial auditory cortex, including putative primary auditory cortex (grid E: $F_{1,8} < 1.0$). To compare SDA and ARM distributions, the amplitudes of each component were normalized over the HP grid. A comparison of these normalized amplitudes showed that ARMs were significantly more laterally distributed (type by M-L interaction in the HP grid: $F_{9,72} = 7.1$, Greenhouse-Geisser $\varepsilon = 0.23$, $P < 0.01$) and slightly more anterior than SDAs (type by A-P interaction: $F_{13,104} = 3.8$, $\varepsilon = 0.19$, $P < 0.05$).

The analysis of the kinetics of activations also revealed a different time course of SDAs and ARMs (**Fig. 4**) that was evident in the analysis of normalized SDA and ARM amplitudes ($F_{10,80} = 3.6$, $\varepsilon = 0.26$, $P < 0.05$). Maximal SDA amplitudes occurred early, 6–8 s after block onset and were followed by amplitude declines throughout the remainder of the block (effect of image number in the HP grid: $F_{14,112} = 14.7$, $\varepsilon = 0.23$, $P < 0.001$). In contrast, ARM amplitude increased gradually throughout the block (effect of image number: $F_{14,112} = 7.7$, $\varepsilon = 0.19$, $P < 0.01$) and did not reach a maximum until after block offset.

SDAs and ARMs also differed in their dependence on stimulus features. SDAs were more prominent in the right hemisphere (hemisphere effect: $F_{1,8} = 16.4$, $P < 0.01$; see **Supplementary Note** online) and were enhanced in the hemisphere contralateral to the stimulated ear (sound location by hemisphere effect: $F_{1,8} = 16.2$, $P < 0.01$), particularly in the small region overlying mesial Heschl's gyrus (grid E: $F_{1,8} = 22.7$, $P < 0.01$; **Fig. 5a**,**b**). In contrast, ARMs were enhanced in the left hemisphere ($F_{1,8} = 9.5$, $P < 0.05$; see **Supplementary Note** online) and were not significantly influenced by ear of delivery, either for the HP array (**Fig. 5b**) or for any of the smaller arrays.

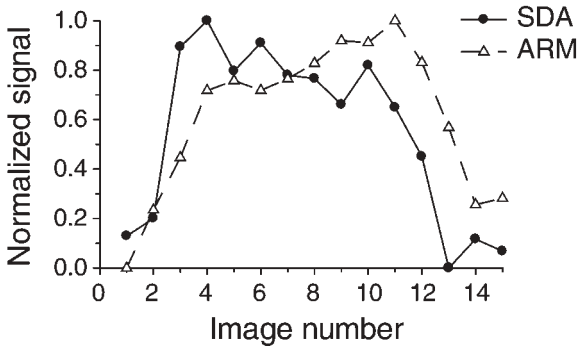

Figure 4 SDA and ARM kinetics. The time course of SDAs (solid line and filled circles) and ARMs (dashed line and open triangles) through one block (images 1–10) and into the next (11–15). Images were acquired every 2 s. Percentage signal change (normalized to maxima/minima for each image sequence) was averaged over data from the HP grid.

SDA locations changed with tone frequency: low frequencies activated posterior, mid-lateral HG and Heschl's sulcus, whereas high frequencies activated anterior-mesial regions of HG ($F_{18,144} = 2.46$, $\varepsilon = 0.19$, $P < 0.08$; see **Fig. 6** and **Supplementary Note** online). This effect derived primarily from a frequency-related medial to lateral displacement over Heschl's gyrus (grid E, frequency by M-L effect, $F_{8,64} = 3.8$, $\varepsilon = 0.39$, $P < 0.05$), with regions sensitive to low frequencies found on more lateral zones of HG (**Fig. 6a**). In contrast, ARM distributions were not significantly influenced by sound frequency, either for the large grid (**Fig. 6b**) or for any of the small grids (see **Supplementary Note** online).

DISCUSSION

Our results suggest a functional dichotomy in human auditory cortex reflected in the different distributions and properties of SDAs and ARMs. SDA distributions were widespread, enhanced in amplitude over the right hemisphere, and they included prominent involvement of mesial auditory cortex. SDAs also changed in distribution with changes in stimulus frequency and location, showing tonotopic displacements with changes in sound frequency and enhanced amplitudes in the hemisphere contralateral to the ear of stimulation. In contrast, ARMs were restricted to lateral cortical regions and were enhanced in amplitude in the left hemisphere. ARM distributions were unaltered by changes in sound frequency or location.

SDAs versus ARMs: tonotopy, spatial tuning and lateralization

SDAs showed a tonotopic organization similar to those reported previously[20,21] with low frequencies represented laterally along Heschl's gyrus and high frequencies represented mesially. Low-frequency tones elicited more extensive activations[22] as would be expected because of the upward frequency spread of cochlear activation to loud sounds[23]. In the current experiment, however, activations to low-frequency tones spanned 20–30 mm over Heschl's gyrus and sulcus (**Fig. 6**), a distance larger than the sizes of putative human ACFs[24,25]. One possible explanation is that low frequencies produced a summed activation over two adjacent ACFs with opposing tonotopic organization[26]. This is consistent with recent results, suggesting a high-to-low mesial field abutting a low-to-high lateral field in mid Heschl's gyrus[17,18]. Although we found no other reliable tonotopic activations, tonotopy in additional fields may have been obscured by intersubject variability in the locations of ACFs and the gyral landmarks used to

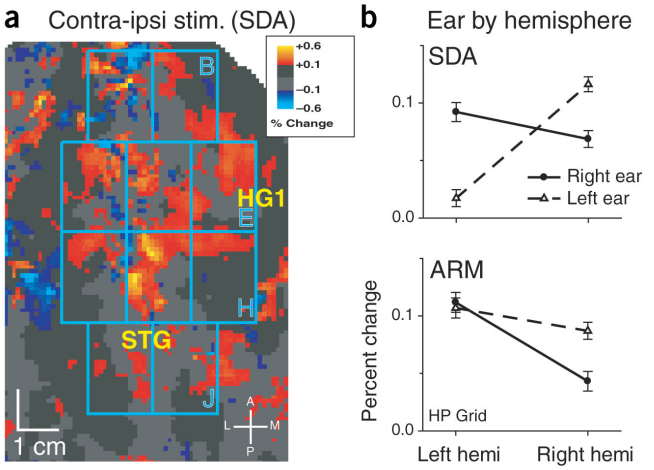

Figure 5 Contralateral versus ipsilateral stimulation. (**a**) Difference in SDAs evoked by contralateral versus ipsilateral stimulation, showing greater activations (red to yellow) in the hemisphere contralateral to the stimulated ear. See **Figure 2c** for further details. (**b**) Ear by hemisphere effects for SDAs (top) and ARMs (bottom) showing contralaterality for SDAs but not ARMs. Data are from the HP grid; error bars designate standard error of the mean (s.e.m.).

align the functional activations (see **Supplementary Fig. 1** and **Supplementary Table 1** online). In contrast to SDAs, ARMs did not show a tonotopic organization in any region of auditory cortex. This suggests that ARMs reflect a coding of auditory objects that is largely independent of the exact pitch of the sounds.

The enhanced SDAs seen in the hemisphere contralateral to the ear of stimulation likely reflect the preponderant contralaterality of spatial receptive fields of neurons in primate auditory cortex[27]. In contrast to results from brain imaging studies of dichotic attention tasks that required attending to sounds in one location and ignoring sounds in another[3,28], in our experiment, ARMs had comparable amplitudes in the hemisphere ipsi- and contralateral to stimulation. This suggests that different neuronal populations in auditory cortex likely participate in spatial and non-spatial auditory attention.

The finding that SDAs were larger in the right hemisphere (see **Supplementary Note** online) is consistent with previous reports of greater right-hemisphere activation in response to simple non-linguistic stimuli such as tones and frequency-modulated sweeps[29,30]. In contrast, ARMs were larger in the left hemisphere (see **Supplementary Note** online), consistent with reports that both linguistic[10,12] and non-linguistic tasks[31] disproportionately enhance activations in left auditory cortex.

SDAs versus ARMs: topographical distribution

Our results suggest that attentionally labile ACFs are primarily restricted to lateral regions of auditory cortex. Lateral fields may be considered hierarchically higher than mesial regions of auditory cortex based on both anatomical[26,32,33] and physiological[34] considerations. Lateral fields have been implicated in a variety of higher-level human auditory perceptual functions, including spatial localization and object identification[35,36]. ARMs were also more anteriorly distributed than SDAs in the current task. Anterior lateral ACFs are known to be involved in the coding of abstract features needed to discriminate auditory signals[36,37], a process that would have been engaged by the sound discriminations required in the current experiment.

SDAs versus ARMs: adaptation functions

Not surprisingly, ARMs and SDAs also differed in adaptation functions. SDAs peaked early and showed rapid adaptation, whereas ARMs increased in amplitude throughout the stimulus block. Rapid habituation of the BOLD response to repeated auditory signals has been previously reported[38]. There is also evidence that this adaptation process is stimulus-specific, since activations are enhanced following occasional deviant sounds even when they are ignored[39]. In our experiment, stimuli at block onset would usually follow previous blocks containing sounds of a different type, frequency and location, or blocks without any auditory stimuli whatsoever. Thus, auditory signals generally changed at block onset, and the sudden and unpredictable change might have transiently captured attention even during visual conditions[40].

The more delayed buildup of ARMs may have reflected both psychological and physiological processes. There were substantial processing delays at block onset, related to decoding the cue, switching attention to the appropriate modality, identifying the type and frequency of stimuli being presented, and storing sound pitch for comparison with subsequent sounds. Enhanced ARM activations late in the block may have reflected contributions from the reduced activations to non-attended sounds due to SDA adaptation. In addition, attention effects late in the block may also have been enhanced by increased demands on memory due to retroactive interference. In any case, the results suggest that ARMs and SDAs show systematic differences in adaptation functions that resemble differences previously reported in ERP studies[41].

Mechanisms of auditory selective attention

Our results demonstrate different topographic distributions and functional properties of ARMs and SDAs, suggesting that these activations are differentially distributed in different ACFs. However, whereas large responses to the unattended loud sounds were restricted to a few regions, small SDAs were elicited throughout auditory cortex. As a result, most areas showing predominant ARMs also showed significant SDAs. Hence, processes engaged to some extent even by nonattended signals appeared to be enhanced by attention in regions showing ARMs.

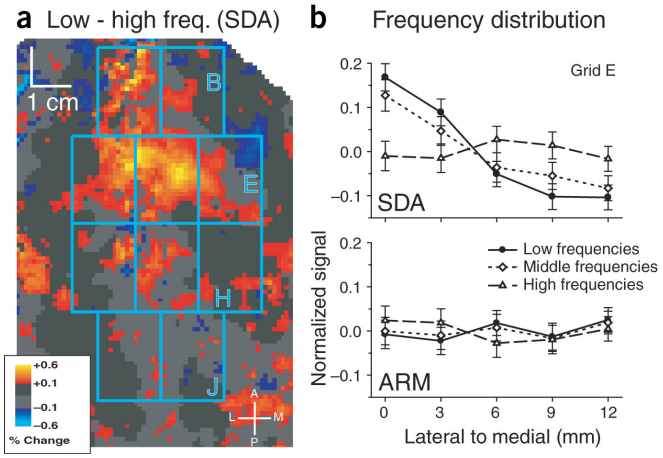

Figure 6 Tonotopy. (**a**) Tonotopic differences between SDAs elicited by 350 and 4,500 Hz (low and high, respectively) centered sounds (red to yellow shows greater activations to low frequencies, blue to cyan shows greater activations to high frequencies). See **Figure 2c** for further details. (**b**) *Z*-score normalized activations (by frequency) showing tonotopic changes in distribution for SDAs (top) but not ARMs (bottom). Data are from grid E; error bars designate s.e.m.

In the visual system, attention amplifies responses to task-relevant stimuli in a manner that is similar to enhancements produced by increasing stimulus contrast[15]. It is possible that auditory attention functions in a similar manner, producing enhancements similar to those produced by increasing sound loudness. Recent brain imaging studies suggest that intensity-related modulations would share several features with ARMs, including reduced frequency specificity in comparison with SDAs and greater amplitudes in the left hemisphere[29]. However, unlike intermodal attention, loudness enhances activations in primary auditory cortex[42,43], suggesting that if attention-related loudness enhancement occurs, its effects are primarily restricted to higher auditory cortical areas.

Alternatively, attention might increase the selectivity of neuronal responses[44]. This would be expected to reduce sequential stimulus adaptation, and enhance activations in lateral regions of auditory cortex that show high levels of adaptation to repeated stimuli[38]. ARMs may also have received contributions from networks involved in auditory target detection, including neural populations in the superior temporal gyrus[45], superior temporal plane and temporal-parietal junction[46].

ARMs might also reflect processing operations, such as short-term auditory memory, that were required in auditory but not visual attention conditions. A number of investigators have previously speculated about common neuronal mechanisms subserving auditory memory and attention[47]. Holding elements in visual short-term memory is associated with increased rates of sustained discharge in neurons that normally fire phasically[48]. In the current experiment, the maintenance of short-term memory for sound features may have similarly increased neuronal discharge in ACFs. If so, this suggests that auditory memory, unlike visual memory[49], may not engage primary sensory cortex and may help to explain the differential contribution of primary cortex to auditory and visual attention effects[50].

CONCLUSION

Our results suggest that the fields of human auditory cortex can be divided into (i) mesial, stimulus-determined regions that process sounds regardless of attentional engagement and (ii) lateral, attentionally labile zones that subserve attentionally dependent, higher-level analyses of sound features. Activations in stimulus-determined regions occurred during visual attention tasks and reflected the physical parameters of the sounds, changing topographically with frequency and location and showing rapid adaptation with sound repetition. In contrast, responses in attentionally labile lateral zones were enhanced by auditory attention, had similar distributions to sounds of different frequencies and locations, and showed amplitudes that increased with sound repetition. A full description of the functional properties of human auditory cortex will require further understanding of the properties of both zones.

Note added in proof: The conference abstract cited in Results has resulted in an in-press publication: Kang, X. *et al.*, Local landmark-based mapping of human auditory cortex. *Neuroimage* (in press).

METHODS

Subjects and tasks. Subjects were 21–43 years of age (5 male and 4 female) with normal hearing and normal corrected visual acuity. All gave informed written consent following VANCHCS Internal Review Board procedures.

Subjects completed four sets of 36, 20-s blocks, including 6 blocks with only visual stimuli and 6 blocks with only auditory stimuli. The experiment included 48 min of data acquisition for each subject. Within a given block, three exemplars from the visual and auditory stimulus classes were used (**Fig. 1**). Attention alternated between auditory and visual conditions, with a cue at fixation ("A" or "V") signaling the attended modality. Block order was otherwise randomized for unimodal or bimodal presentation, sound frequency, ear of delivery, sound type, visual stimulus type and visual stimulus location. Targets (12–14% probability) were sound repetitions in auditory attention blocks, and in the different visual attention conditions, targets were repetitions of either visual shape or direction of dot motion (four diagonal directions). Targets required a speeded button press response from subjects.

Stimuli. Auditory and visual stimuli were 200 ms in duration. Stimulus onset asynchronies (SOAs) varied randomly between 245 and 755 ms and were independent in auditory and visual modalities. Sounds were tones or band-passed noise bursts (4 semitones wide) with rise/fall times of 5 ms. They varied over an eight-semitone (0.67 octave) range centered on low, medium or high frequencies (350, 1,400 or 4,500 Hz). Sound type, frequency and location (either left or right ear) remained fixed throughout each block. These factors varied randomly and exhaustively on successive blocks. Sounds were presented at a mean rate of 2/s. Sounds were matched in RMS level and presented at 95 dB SPL (approximately 78 dB SPL at the ear drum after attenuation through Etymotic musician's ear plugs with uniform 17 dB attenuation across the frequency spectrum). Scanner noise (112 dB SPL) passed through three levels of attenuation: (1) foam padding around the subject's head and scanner bore, (2) modified Koss ESP-950 electrostatic, circumaural headphones and (3) earplugs. After this attenuation, the scanner noise was psychophysically matched to a playback of scanner noise at 75 dB SPL. Background binaural white noise was presented at 92 dB SPL (approximately 75 dB after attenuation through the earplugs) to mask the scanner noise and to limit the frequency splatter of loud sounds.

Visual stimuli were rear-projected onto a screen at the subject's feet with a high-luminance LCD projector and were viewed through a mirror mounted on the MR head coil. Stimuli were three different white shapes (see **Fig. 1**) or moving random dot patterns (4 diagonal directions) presented along either the left or right diagonal (upper left and lower right or lower left and upper right quadrants) of a darkened background. Visual stimulus type and location were fixed during each block but varied randomly and exhaustively between blocks. Presentation software (www.neurobs.com, version 0.60) was used to deliver the stimuli. The stimuli and experiment control files can be viewed and downloaded at http://nbs.neuro-bs.com/ex_files/expt_view?id=33.

Imaging methods. Brain imaging was performed with a Philips Eclipse 1.5 T scanner and Philips head coil. Head movement was restrained with foam padding. Twenty EPI axial images were designed to cover the entire cerebral cortex (128 × 128 × 20 matrix, 1.87 × 1.87 × 5 mm resolution, 1 mm gap in axial slices, TR = 2 s, TE = 40 ms, f.o.v. = 240 mm, flip angle = 90°). The first ten EPI images of each imaging run were discarded, as this represented the time for magnetization to reach a steady state and for subject performance to stabilize. Anatomical images were acquired separately (3D T1-weighted, coronal 256 × 212 × 256 voxel matrix, 0.94 × 1.13 × 0.94 mm resolution, TR = 15 ms, TE = 4.47 ms, flip angle = 35°).

Anatomical image sets were resliced to 1 mm^3, inflated, cut and flattened (**Fig. 2a**,**b**) using FreeSurfer software (http://surfer.nmr.mgh.harvard.edu). On the flattened superior temporal lobe, we selected five fiducial points for the landmark-based anatomical normalization (**Fig. 2b**). Mean locations were calculated across subjects, and a linear least-square-error affine transformation was used to warp individual anatomical and functional data onto this common anatomical coordinate system. All of the individual functional EPI images were co-registered and resliced into the 1 mm^3, high-resolution anatomical space using SPM99 software (http://www.fil.ion.ucl.ac.uk/spm). The data used for further analysis were extracted from these high-resolution functional images.

Data analysis. The data were quantified using analysis grids projected onto the inflated cortical surface (cyan boxes A–J in **Fig. 2c**). A large Heschl's gyrus, planum temporale grid (30 × 42 mm) was positioned as shown and contained four small grids (D, E, G and H; see dark blue dashed line in **Fig. 2c**). Grid E overlays the mesial portion of Heschl's gyrus (corresponding to primary auditory cortex[19]). Six additional small grids, each 15 mm in width and 21 mm in length, were positioned over the flattened temporal cortex patch to cover the full extent of auditory cortex.

Mean percent activation measures were obtained for the 3 × 3 mm elements of each grid (white boxes in grid I, **Fig. 2c**) using images 2–12 within a block. The data were analyzed using repeated-measures ANOVA with Greenhouse-Geisser correction, using the CLEAVE program (www.ebire.org/hcnlab). An initial omnibus analysis was performed on the Heschl's gyrus/planum temporale (HP) grid composed of four smaller grids. Significant effects were identified in the HP grid, and the spatial extent of these effects was examined in the smaller grids. Significant main effects and up to three-way interactions are reported. Additional 4-, 5- and 6-way interactions are not discussed as they rarely reached significance, could not easily be corrected for violations of sphericity, and were difficult to interpret.

Based on the kinetics of SDAs and ARMs (**Fig. 4**) maximal SDAs were observed in frames 3–8 and maximal ARMs in frames 7–12. The figures show signal magnitudes from these peak-activation ranges with display thresholds set at 0.1%.

Note: Supplementary information is available on the Nature Neuroscience website.

ACKNOWLEDGMENTS

Supported by grant DC005814 from the National Institutes of Health (National Institute on Deafness and Other Communication Disorders), by the Department of Veterans Affairs Research Service, a MIND (Medical Investigation of Neurodevelopmental Disorders) Institute fellowship to C.P., the Academy of Finland (grants 49126 and 102316) and the Institut National de la Santé et de la Recherche Médicale. We thank T. Herron for the development of statistical tools, and G. Recanzone, D. Swick and the anonymous reviewers for comments on previous versions of the manuscript.

COMPETING INTERESTS STATEMENT

The authors declare competing financial interests (see the *Nature Neuroscience* website for details).

Received 10 December 2003; accepted 29 March 2004
Published online at http://www.nature.com/natureneuroscience/

1. Woods, D.L., Alho, K. & Algazi, A. Intermodal selective attention I: Effects on event-related potentials to lateralized auditory and visual stimuli. *Electroencephalogr. Clin. Neurophysiol.* **82**, 341–355 (1992).
2. Alho, K., Woods, D.L., Algazi, A. & Näätänen, R. Intermodal selective attention II. Effects of attentional load on processing auditory and visual stimuli in central space. *Electroencephalogr. Clin. Neurophysiol.* **82**, 356–368 (1992).
3. Alho, K. *et al.* Selective tuning of the left and right auditory cortices during spatially directed attention. *Brain Res. Cogn. Brain Res.* **7**, 335–341 (1999).
4. Woodruff, P.W. *et al.* Modulation of auditory and visual cortex by selective attention is modality-dependent. *Neuroreport* **7**, 1909–1913 (1996).
5. Woldorff, M.G. *et al.* Modulation of early sensory processing in human auditory cortex during auditory selective attention. *Proc. Natl. Acad. Sci. USA* **90**, 8722–8726 (1993).
6. Alcaini, M., Giard, M.H., Thevenet, M. & Pernier, J. Two separate frontal components in the N1 wave of the human auditory evoked response. *Psychophysiology* **31**, 611–615 (1994).
7. Woods, D.L. & Alain, C. Conjoining three auditory features: an event-related brain potential study. *J. Cogn. Neurosci.* **13**, 493–509 (2001).
8. Woods, D.L., Hillyard, S.A., Courchesne, E. & Galambos, R. Electrophysiological signs of split-second decision-making. *Science* **207**, 655–657 (1980).
9. Tzourio, N. *et al.* Functional anatomy of human auditory attention studied with PET. *Neuroimage* **5**, 63–77 (1997).
10. Jäncke, L., Mirzazade, S. & Shah, N.J. Attention modulates activity in the primary and the secondary auditory cortex: a functional magnetic resonance imaging study in human subjects. *Neurosci. Lett.* **266**, 125–128 (1999).
11. Pugh, K.R. *et al.* Auditory selective attention: an fMRI investigation. *Neuroimage* **4**, 159–173 (1996).
12. Grady, C.L. *et al.* Attention-related modulation of activity in primary and secondary auditory cortex. *Neuroreport* **8**, 2511–2516 (1997).
13. Binder, J.R. *et al.* Human temporal lobe activation by speech and nonspeech sounds. *Cereb. Cortex* **10**, 512–528 (2000).
14. Rauschecker, J.P. Cortical processing of complex sounds. *Curr. Opin. Neurobiol.* **8**, 516–521 (1998).
15. Desimone, R. Visual attention mediated by biased competition in extrastriate visual cortex. *Phil. Trans. R. Soc. London B Biol. Sci.* **353**, 1245–1255 (1998).
16. Dale, A.M., Fischl, B. & Sereno, M.I. Cortical surface-based analysis I. Segmentation and surface reconstruction. *Neuroimage* **9**, 179–194 (1999).
17. Talavage, T.M. *et al.* Tonotopic organization in human auditory cortex revealed by progressions of frequency sensitivity. *J. Neurophysiol.* **91**, 1282–1296 (2004).
18. Formisano, E. *et al.* Mirror-symmetric tonotopic maps in human primary auditory cortex. *Neuron* **40**, 859–869 (2003).
19. Rademacher, J. *et al.* Probabilistic mapping and volume measurement of human primary auditory cortex. *Neuroimage* **13**, 669–683 (2001).
20. Schönwiesner, M., Von Cramon, D.Y. & Rübsamen, R. Is it tonotopy after all? *Neuroimage* **17**, 1144–1161 (2002).
21. Talavage, T.M., Ledden, P.J., Benson, R.R., Rosen, B.R. & Melcher, J.R. Frequency-dependent responses exhibited by multiple regions in human auditory cortex. *Hear. Res.* **150**, 225–244 (2000).
22. Bilecen, D., Scheffler, K., Schmid, N., Tschopp, K. & Seelig, J. Tonotopic organization of the human auditory cortex as detected by BOLD-FMRI. *Hear. Res.* **126**, 19–27 (1998).
23. Phillips, D.P., Semple, M.N., Calford, M.B. & Kitzes, L.M. Level-dependent representation of stimulus frequency in cat primary auditory cortex. *Exp. Brain Res.* **102**, 210–226 (1994).
24. Wallace, M.N., Johnston, P.W. & Palmer, A.R. Histochemical identification of cortical areas in the auditory region of the human brain. *Exp. Brain Res.* **143**, 499–508 (2002).
25. Rivier, F. & Clarke, S. Cytochrome oxidase, acetylcholinesterase, and NADPH-diaphorase staining in human supratemporal and insular cortex: evidence for multiple auditory areas. *Neuroimage* **6**, 288–304 (1997).
26. Kaas, J.H., Hackett, T.A. & Tramo, M.J. Auditory processing in primate cerebral cortex. *Curr. Opin. Neurobiol.* **9**, 164–170 (1999).
27. Recanzone, G.H. Spatial processing in the auditory cortex of the macaque monkey. *Proc. Natl. Acad. Sci. USA* **97**, 11829–11835 (2000).
28. Jäncke, L., Specht, K., Shah, J.N. & Hugdahl, K. Focused attention in a simple dichotic listening task: an fMRI experiment. *Brain Res. Cogn. Brain Res.* **16**, 257–266 (2003).
29. Brechmann, A., Baumgart, F. & Scheich, H. Sound-level-dependent representation of frequency modulations in human auditory cortex: a low-noise fMRI study. *J. Neurophysiol.* **87**, 423–433 (2002).
30. Celsis, P. *et al.* Differential fMRI responses in the left posterior superior temporal gyrus and left supramarginal gyrus to habituation and change detection in syllables and tones. *Neuroimage* **9**, 135–144 (1999).
31. Gaab, N., Keenan, J.P. & Schlaug, G. The effects of gender on the neural substrates of pitch memory. *J. Cogn. Neurosci.* **15**, 810–820 (2003).
32. Kosaki, H., Hashikawa, T., He, J. & Jones, E.G. Tonotopic organization of auditory cortical fields delineated by parvalbumin immunoreactivity in macaque monkeys. *J. Comp. Neurol.* **386**, 304–316 (1997).
33. Hackett, T.A., Preuss, T.M. & Kaas, J.H. Architectonic identification of the core region in auditory cortex of macaques, chimpanzees, and humans. *J. Comp. Neurol.* **441**, 197–222 (2001).
34. Rauschecker, J.P. & Tian, B. Mechanisms and streams for processing of "what" and "where" in auditory cortex. *Proc. Natl. Acad. Sci. USA* **97**, 11800–11806 (2000).
35. Alain, C., Arnott, S.R., Hevenor, S., Graham, S. & Grady, C.L. "What" and "where" in the human auditory system. *Proc. Natl. Acad. Sci. USA* **98**, 12301–12306 (2001).
36. Wessinger, C.M. *et al.* Hierarchical organization of the human auditory cortex revealed by functional magnetic resonance imaging. *J. Cogn. Neurosci.* **13**, 1–7 (2001).
37. Warren, J.D. & Griffiths, T.D. Distinct mechanisms for processing spatial sequences and pitch sequences in the human auditory brain. *J. Neurosci.* **23**, 5799–5804 (2003).
38. Jäncke, L. *et al.* The time course of the BOLD response in the human auditory cortex to acoustic stimuli of different duration. *Brain Res. Cogn. Brain Res.* **8**, 117–124 (1999).
39. Opitz, B., Rinne, T., Mecklinger, A., Von Cramon, D.Y. & Schröger, E. Differential contribution of frontal and temporal cortices to auditory change detection: fMRI and ERP results. *Neuroimage* **15**, 167–174 (2002).
40. Escera, C., Alho, K., Winkler, I. & Näätänen, R. Neural mechanisms of involuntary attention to acoustic novelty and change. *J. Cog. Neurosci.* **10**, 590–604 (1998).
41. Woods, D.L. in *Event-Related Brain Potentials: Issues and Interdisciplinary Vantages* (eds. Rohrbaugh, J.W., Johnson, R. & Parasuraman, R.) 178–209 (Oxford Univ. Press, New York, 1990).
42. Jäncke, L., Shah, N.J., Posse, S., Grosse-Ryuken, M. & Muller-Gartner, H.W. Intensity coding of auditory stimuli: an fMRI study. *Neuropsychologia* **36**, 875–883 (1998).
43. Bilecen, D., Seifritz, E., Scheffler, K., Henning, J. & Schulte, A.C. Amplitopicity of the human auditory cortex: an fMRI study. *Neuroimage* **17**, 710–718 (2002).
44. Murray, S.O. & Wojciulik, E. Attention increases neural selectivity in the human lateral occipital complex. *Nat. Neurosci.* **7**, 70–74 (2004).
45. Kiehl, K.A., Laurens, K.R., Duty, T.L., Forster, B.B. & Liddle, P.F. Neural sources involved in auditory target detection and novelty processing: an event-related fMRI study. *Psychophys.* **38**, 133–142 (2001).
46. Downar, J., Crawley, A.P., Mikulis, D.J. & Davis, K.D. The effect of task relevance on the cortical response to changes in visual and auditory stimuli: an event-related fMRI study. *Neuroimage* **14**, 1256–1267 (2001).
47. Cowan, N. Evolving conceptions of memory storage, selective attention, and their mutual constraints within the human information-processing system. *Psychol. Bull.* **104**, 163–191 (1988).
48. Desimone, R. Neural mechanisms for visual memory and their role in attention. *Proc. Natl. Acad. Sci. USA* **93**, 13494–13499 (1996).
49. Kosslyn, S.M., Thompson, W.L., Kim, I.J. & Alpert, N.M. Topographical representations of mental images in primary visual cortex. *Nature* **378**, 496–498 (1995).
50. Martinez, A. *et al.* Involvement of striate and extrastriate visual cortical areas in spatial attention. *Nat. Neurosci.* **2**, 364–369 (1999).